



## Development of Mobile Device for Gamma Radiation Measurement utilizing LoRa as the Communication Means

I Putu Susila<sup>1\*</sup>, Agung Alfiansyah<sup>2</sup>, Istofa<sup>1</sup>, Sukandar<sup>1</sup>, Budi Santoso<sup>1</sup>, Suratman<sup>3</sup>

<sup>1</sup>Center for Nuclear Facility Engineering, National Nuclear Energy Agency of Indonesia, Tangerang Selatan, Indonesia

<sup>2</sup>Computer System Engineering, Prasetiya Mulya University, BSD City, Indonesia

<sup>3</sup>Center for Informatics and Nuclear Strategic Zone Utilization, National Nuclear Energy Agency of Indonesia, Tangerang Selatan, Indonesia

### ARTICLE INFO

#### Article history:

Received: 13 May 2019

Received in revised form: 22 July 2019

Accepted: 23 July 2019

#### Keywords:

Radiation monitoring  
Decision Support System

Mobile

LoRa

GPS

### ABSTRACT

Public protection is one of important issues when operating nuclear facility. In case of accident occurs, the facility owner and related organizations shall make decision whether to evacuate people or not, based on the level of the accident and radiation dose rate released to the environment. In this study, as part of the decision support system for nuclear emergency response, a prototype of mobile radiation measurement system has been developed. The device consists of Geiger-Muller (GM)-based radiation measurement board, Global Positioning System (GPS) module, microcontroller board, and low power LoRa module for communication. Radiation dose rate along with its geoposition were recorded and sent to base station equipped with LoRa gateway for connecting LoRa network to TCP/IP-based network. The measurement data is then published to storage server using Message Queuing Telemetry Transport (MQTT) protocol. Power consumption, measurement of counter/timer accuracy, communication ranges testing, and radiation dose rate measurement were performed around Puspipetek area to demonstrate the functionality of the system.

© 2019 Tri Dasa Mega. All rights reserved.

### INTRODUCTION

Radiation is the emission of energy through a material or space in the form of particles or electromagnetic waves. Usually, radiation is categorized into non-ionizing and ionizing radiation. Examples of non-ionizing radiation are radio waves, infrared, and visible light, where these types of radiation are unable to cause ionizing effects when absorbed by objects or materials. Conversely, ionizing radiation is a radiation that possess enough energy to ionize the object or material it passes through. Examples of ionizing radiation are X-rays, gamma rays, alpha particles, and so on. In general, the term radiation usually refers to ionizing radiation.

In our daily life, radiation exists around us, and this radiation is called natural radiation. There are also man-made radiation source such as x-ray used for medical purpose and gamma radiation source used in industrial application. Apart from natural and man-made sources, radiation may also be generated due to radiological emergencies such as the use of dirty bombs (devices containing conventional explosives along with radioactive substances), accidents when transporting radioactive substances, and nuclear emergencies namely accidents that occur at nuclear facilities, such as the incident of the Fukushima Dai'ichi Nuclear Reactor in 2011 [1].

Uncontrolled exposure to radiation can cause adverse effects on the environment and increase health risks for the community. Therefore, if there were to be a radiological or nuclear emergency, in order to minimize the effect, action needs to be

\* Corresponding author. Tel./Fax.: +62-217560896

E-mail: [putu@batan.go.id](mailto:putu@batan.go.id)

DOI: [10.17146/tdm.2019.21.2.5432](https://doi.org/10.17146/tdm.2019.21.2.5432)

taken in accordance with the level of emergency. Such actions can take the form of immediate protection from the affected area, evacuation, individual decontamination, provision of respiratory protection, and prohibition on consumption of foods potentially contaminated by radioactive material. The decision could be taken based on the calculation by a decision support system [2, 3] and measurement result of radiation dose in the affected area. In the latter case, a mobile radiation monitoring system is required.

Currently, several wireless technologies such as Bluetooth, Wi-Fi, cellular network, and Long Range (LoRa) radio [4, 5] are available for such system. Compared to Bluetooth and Wi-Fi, which normally has small coverage area unless expanded using special antenna, the coverage area of cellular network is nationwide. However, the network especially the base station depends on the availability of grid power. Thus, in case of emergency situation, the network may not properly function due to lack of power source.

LoRa is relatively new technology proposed by SemTech and now developed by LoRa Alliance [6]. The communication system is based on proprietary modulation scheme which uses Chirp Spread Spectrum technique. The technology supports variable data rate and its throughput can be set accordingly to trade-off for coverage range, or robustness, or energy consumption. Several applications utilizing this technology have been reported, and shown to be able to support long range communication [4–7].

In this study, we would like to develop a mobile radiation monitoring system that can be used to monitor radiation dose rate, especially gamma radiation. The device is a part of a decision support system for nuclear emergency response. The objectives of this study are to develop a prototype, measure its characteristics, and investigate the possibility of utilization of LoRa communications in real field around Serpong Nuclear Facility.

## METHODOLOGY

### System Overview

Proposed system architecture is shown in Fig. 1(a). The system consists of mobile radiation monitoring, communication module, LoRa network to TCP/IP gateway, Message Queuing Telemetry Transport (MQTT) broker, and database. The

device uses LoRa module to send field measurement data through LoRa network. Measurement data then being sent to LoRa-TCP/IP gateway which acts as a bridge between LoRa network and TCP/IP based network. The gateway consists of programmable Arduino-based microcontroller [8, 9] and TCP/IP router utilizing OpenWRT [10]. Data received through LoRa network is being parsed in the microcontroller, and then being published to specific communication channel in MQTT broker. Finally, the broker sends the data to all subscribers which subscribe to the same channel used by the gateway. In this study, only one subscriber which saves the measurement data to PostgreSQL database was developed.

The proposed system architecture is known as publish-subscribe (Pub-Sub) communication model over MQTT protocol. Conceptually, Pub-Sub model is shown in Fig. 1(b). As shown in the figure, every MQTT client, data processing application or field device such as radiation monitoring station and meteorological tower, needs to connect to a broker before communicating with other clients. The broker accepts published messages being sent to a specific channel and then delivers them to all the interested consumers (subscribers) subscribing to the channel. According to benchmark by ScalAgent Distributed Technologies using Intel Core2Duo CPU E8400 3.00GHz server having 4GB memory, when configured with no acknowledgement, no persistence, Mosquitto broker can handle up to 60,000 messages per second (payload size is fixed and set to 64 bytes), while another commercial MQTT broker can handle up to 100,000 messages per second [11]. This performance is sufficient for handling sensors data from radiation and meteorological monitoring stations which typically sending data to the server in the order of several seconds or even minutes.

Utilizing publish-subscribe communication model enables us to easily extent the system, e.g. adding an early warning system [12], or storing the measurement data to existing radiation monitoring system [13, 14] will be easy. In this study, the database and subscriber application are developed in personal computer. In case of emergency situation which may damage the electrical grid, the database and application should be developed to battery power-embedded computer.

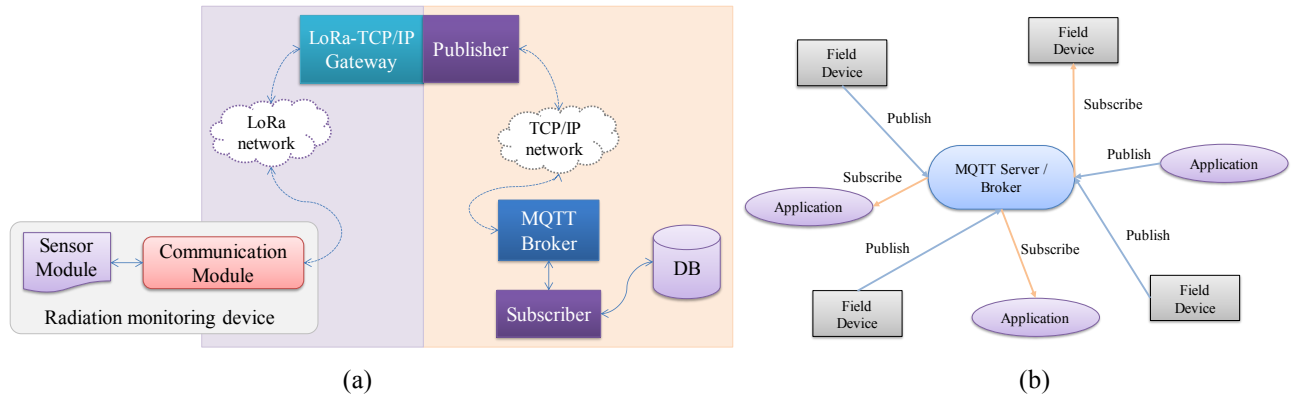


**Fig. 1.** System overview, (a) architecture of mobile radiation monitoring system, (b) Publish-Subscribe communication model utilizing MQTT Protocol

**Mobile Radiation Monitoring Device**

Block diagram of radiation monitoring device is shown in Fig. 2. The device consists of communication module and sensor module. Fig. 2(a) shows the block diagram for communication module. An Arduino-based microcontroller is used to acquire data from sensor module and position from GPS module through universal asynchronous receiver-transmitter (UART). The data is then being sent to LoRa communication module through serial peripheral interface (SPI). In current prototype, we used commercially available Arduino board and shields to construct the module.

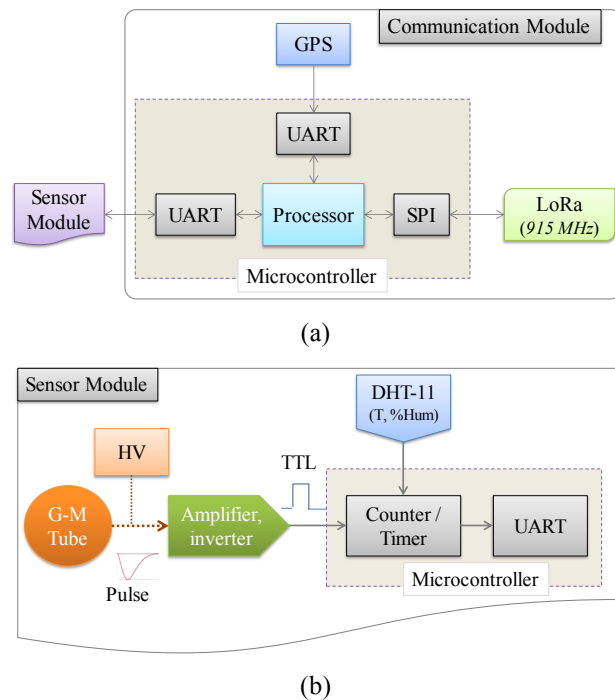


**Fig. 2.** Battery-powered radiation monitoring device which consists of (a) LoRa-based communication module with GPS, and (b) radiation, temperature and relative humidity measurement module

Block diagram of the sensor module is shown in Fig. 2(b). It consists of G-M pancake detector, high voltage supply module, electronic circuit for converting detector signal to 5V transistor-transistor logic (TTL) signal, DHT-11 temperature and relative humidity sensor, and Arduino-based microcontroller for counter/timer and communication. The resolution of the counter is 16-bits while timer resolution is 8-bits. Instead of dedicated component for counter/timer, a microcontroller was chosen to simplify the electronic circuit. This module was designed and implemented into a dedicated printed circuit board (PCB) and then being connected to communication module through UART.

**Testing and Data Analysis**

The prototype of mobile radiation monitoring device was developed, constructed, and tested in our laboratory. Device power consumption was measured continuously for certain period using Fluke multimeter. During measurement, the value displayed in multimeter is recorded in a video, and then recorded manually into a spreadsheet for further analysis.

Counter/timer that counts radiation events generated by G-M detector was tested using function generator. Digital signal with frequency between 10 Hz – 30 kHz was generated by the function generator, and then used as input pulse to the counter. The aim of this test is to determine the accuracy of the counter/timer. In the microcontroller, counter and timer are independent peripheral separated from the processor. In this prototype, we use interrupt to count the events. The accuracy is determined by the clock source for the timer, and for this prototype, a 16 MHz crystal oscillator is being used as the clock source. Thus,

relatively high accuracy is expected for the counter and timer. To measure the accuracy, we used discrepancy between the frequency of digital signal generated by function generator and counter value within one second period.

The functionality of the sensor board is tested by measuring air temperature and relative humidity in room temperature condition. Furthermore, for testing radiation detection system, we apply Cs-137 standard check source on detector then measure the dose rate in count per minute (CPM). Finally, to determine communication ranges and GPS functionality, a field test around our office in Puspiptek Serpong was conducted. During testing, all the data is recorded in database for further analysis.

**RESULTS AND DISCUSSION**

**Developed Hardware**

Battery-powered radiation monitoring device which was developed in this study is shown in Fig. 3. The device consists of pancake type G-M tube manufactured by Saint-Gobain Crystals, self-developed sensor module, and stackable communication module. The sensor module consists of manually adjustable high voltage power supply circuit, DHT-11 temperature and humidity sensor, amplifier and inverter circuit connected to the G-M tube, ATmega328p microcontroller running at 16MHz clock speed, and switching DC-DC converter which supply 5VDC to the circuit. Furthermore, the communication module consists of Arduino Uno Rev3 [8], SIM908 module which is a Quad-Band GSM/GPRS module combined with GPS technology for satellite navigation (in this study, only the GPS part is used), and 915 MHz LoRa module.

The developed device requires 9VDC as its power source, and currently, 6 (sixes) D cell batteries are used to power it. During operation, measured current was  $221.2 \pm 3.8$  mA (25 seconds measurement,  $n = 50$ ) or in term of power rating, it is approximately equal to 2W. Further measurement is needed to get detail power consumption profile up to component level, e.g. power consumption by the microcontroller chip, LED indicators, HV supply unit, LoRa module, and GPS module. The information will be used to improve existing hardware design, such as lowering supply voltage, reducing clock speed of the microcontroller, and removing unnecessary component. Furthermore, development of smart algorithm for communication and power management may be needed to get a prototype that consumes less power [15, 16].

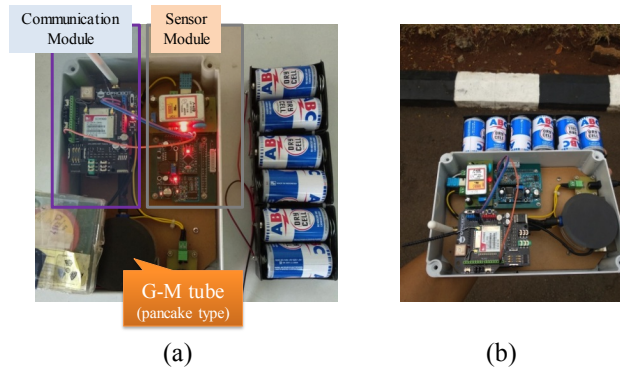


**Fig. 3.** Developed battery-powered radiation, temperature and relative humidity measurement device. Figure (a) shows each module, pancake type G-M tube and radiation check source, while (b) shows device during field testing around our office

**Counter/Timer Accuracy**

Fig. 4 shows the result of counter and timer accuracy testing. In Fig. 4(a), x-axis is frequency of pulse (used as counter input) produced by function generator, while y-axis is pulse count per second. Note that both x and y-axis are in logarithmic scale. Ideally, both input pulse frequency and pulse count should be the same. However, in reality the pulse count is slightly lower than the frequency.

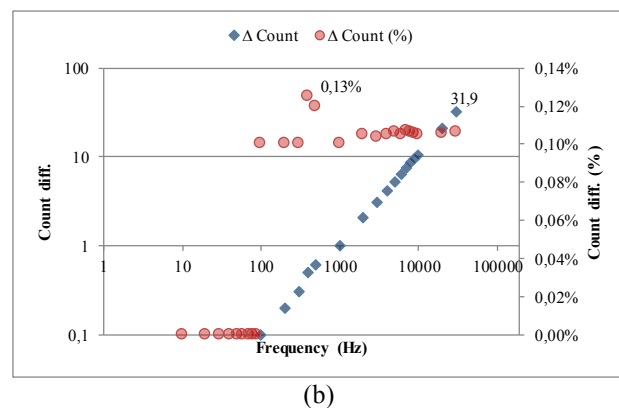
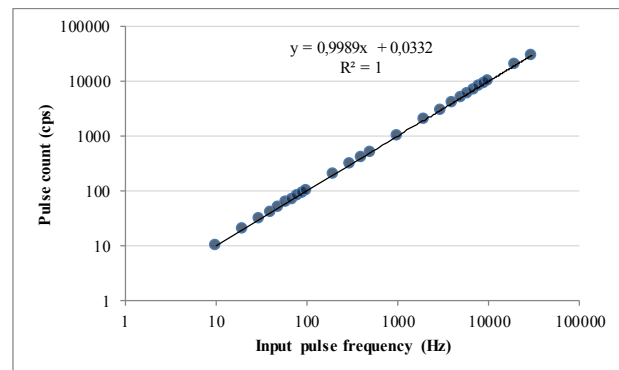


**Fig. 4.** Counter/timer accuracy, (a) relation between input pulse generated by function generator with its counting result, (b) count difference in cps and percent at certain frequency

Fig. 4(b) shows the difference between input pulse frequency and pulse count produced by counter. In the figure, x-axis and primary y-axis are in logarithmic scale, while secondary y-axis is in linear scale. As shown in the figure, when the frequency is less than 100 Hz, the pulse count is equal to input pulse frequency, and as the frequency increases, the discrepancy between the two is also increased. The maximum difference value is 31.9 counts per second when the frequency is 30 kHz. If the difference is expressed as the percentage against input pulse frequency, the value is almost constant with the maximum value of 0.13 %.

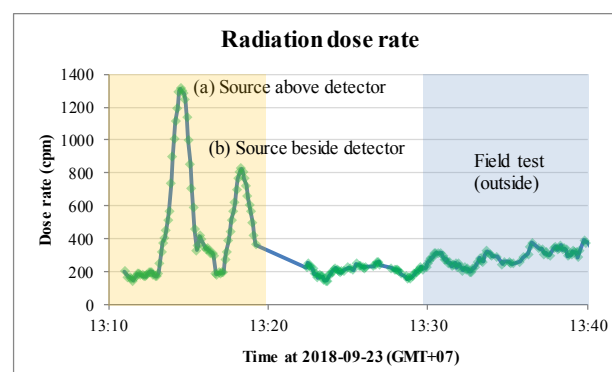
The specification of G-M detector used in our prototype specifies that Cs-137 gamma sensitivity is 65 cps per mR/hr or 65 cps per 10,000 nSv/h. Previous study [13] shows that the average environmental gamma dose rate around Serpong nuclear facility is 84-99 nSv/h. This dose rate is equal to 0.5460 - 0.6435 cps for G-M detector used in current prototype. Thus, the dose rate calculation error caused by counter/timer inaccuracy is negligible.

### Functional Test

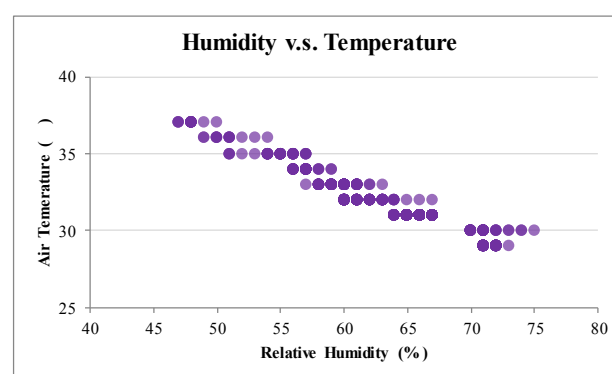
Measured radiation dose rate is shown in Fig. 5(a). In the figure, x-axis is time stamp, while y-axis is radiation dose rate in counts per minute (CPM). Peak (a) in the figure shows measured dose rate when Cs-137 check source is placed above the detector window, peak (b) is the dose rate when the check source is placed beside the detector window, and the other case when no source present around the detector both inside and outside building. Maximum detection efficiency is reached when the radiation source is placed straight to the detector window i.e. as shown in peak (a) in which the radiation dose rate is higher compared to other cases.

The result of temperature and humidity measurement is shown in Fig. 5(b). DHT-11 sensor is used to measure temperature and humidity. The measurement range of the sensor is 20-90% RH and 0-50 °C, while the humidity accuracy is  $\pm 5\%$  RH and the temperature accuracy is  $\pm 2$  °C. These sensors were added to anticipate the change in radiation measurement due to diurnal effect [17]. Relative humidity indicates the percentage of actual amount of water vapour in the air. Chart in Fig. 5 (b) shows that relative humidity is increased when air temperature decreased (inversely related) which is widely known [16]. In relation to air temperature, moisture holding capacity of the air depends on its temperature. The holding capacity increases when temperature increases. As the moisture holding

capacity increases the relative humidity decreases, provided no moisture is added to the air [18–20].



(a)



(b)

**Fig. 5.** Measurement result, (a) radiation dose rate in CPM, (b) relation between relative humidity and air temperature

The result of field test (Fig. 3 (b)) around our office at Serpong Nuclear Facility is shown in Fig. 6. The frequency of the LoRa module was 915 MHz, while the bandwidth was 125 kHz. Measurement data that includes longitude, latitude, mean sea level (MSL), radiation dose rate, air temperature, and relative humidity was sent to storage computer through LoRa to TCP/IP gateway located at the second floor of our office building. The data is sent periodically every 5 seconds. Measured radiation data is shown in Fig. 5(a) between 13:30-13:40 (GMT+07).

The test route passed through open field and meteorological monitoring station. During testing, we brought the device by foot in relatively constant speed. Ideally, if no transmission error occurs, the interval between location points (longitude, latitude) should be constant. However, as shown in Fig. 6, at some places e.g. (A) and (B), several points were missing. In this case, either GPS coordinate is not fixed or the data transmitted through LoRa was unable to reach the Gateway. The transmission power, type of antenna, and the presence of obstacle such as tree or concrete wall

are several factors that may affect the coordinate validity and data transmission.

The results presented in Fig. 3-Fig. 6 demonstrate that the prototype worked as expected. Device testing using Cs-137 check source show that gamma radiation dose rate can be measured properly. In the future, device calibration is needed to convert radiation dose rate measured in CPM to appropriate unit such as  $\mu\text{Sv/h}$ . In addition to radiation dose rate, temperature and relative humidity were measured successfully. However, the DHT-11 sensor has limited accuracy, and as the result, the plotted measurement data is quite rough (Fig. 5(b)). In the next prototype, sensor which has better resolution should be used.

Result of LoRa communication range testing shows that longest distance was about 200 m (Fig.

6). With this distance, LoRa communication can be used to replace existing communication means for transferring meteorological data from station to data centre. Previous studies [5-6] show that LoRa can achieve longer communication distance and wider coverage area. In order to extent the communication range, more detail investigation such as measurement of signal quality, variation of bandwidth, as well as field testing at wider area will be performed. Furthermore, in Indonesian context, the frequency band for LoRa communication is yet to be allocated by Ministry of Communication and Informatics. In the future, when LoRa related regulation is released by the government, the frequency must be adjusted accordingly.

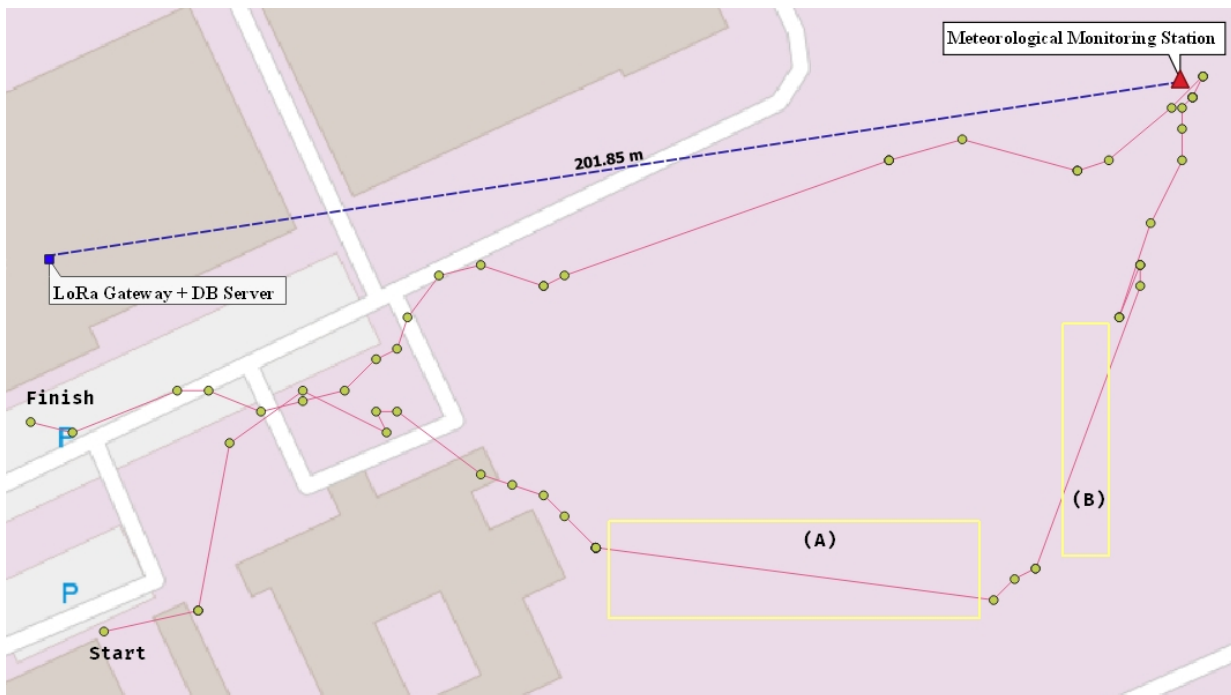


Fig. 6. Routes and measurement point during field test around our office

## CONCLUSION

A prototype of mobile radiation measurement system has been developed. The prototype developed as part of a decision support system for nuclear emergency response. The device consists of Geiger-Muller (GM)-based radiation dose rate, temperature and relative humidity measurement sensors, GPS module, microcontroller board and LoRa module for data communication. Measurement of power consumption showed that the prototype power rating was 2W, and embedded counter/timer discrepancy was less than 0.13%. During field testing around our office at Puspiptek Serpong, radiation dose rate along with its geo-position were recorded and being sent to base station equipped with LoRa gateway for connecting LoRa network to TCP/IP-based network. The measurement data is then published to storage server using MQTT protocol. Field test result demonstrates the functionality of the developed prototype. In the future, further improvement to reduce power consumption, and detail measurement to accurately determine LoRa coverage area are needed.

## ACKNOWLEDGMENT

This study is supported by *Insentif Riset Sistem Inovasi Nasional* (INSINAS), *Kementerian Riset, Teknologi, dan Pendidikan Tinggi Republik Indonesia* (Kemenristekdikti) grant number 4/INS-2/PPK/E4/2018. The authors also would like to thank the members of the Nuclear Instrumentation Division, Center for Nuclear Facility Engineering-BATAN for their technical support and assistance.

## REFERENCES

- Kinoshita N., Sueki K., Sasa K., Kitagawa J., Ikarashi S., Nishimura T., et al. Assessment of individual radionuclide distributions from the Fukushima nuclear accident covering central-east Japan. *Proc. Natl. Acad. Sci.* 2011. **108**(49):19526–9.
- Ehrhardt J., Päsler-Sauer J., Schüle O., Benz G., Rafat M., Richter J. Development of RODOS\*, A Comprehensive Decision Support System for Nuclear Emergencies in Europe - An Overview. *Radiat. Prot. Dosimetry.* 2017. **50**(2–4):195–203.
- Hoe S., Mueller H. ARGOS - a decision support system for nuclear emergencies. in: *International Symposium on Off-site Nuclear Emergency Management.* Salzburg. 2003. p. 170.
- Vangelista L., Zanella A., Zorzi M. Long-Range IoT Technologies: The Dawn of LoRa™. Springer, Cham; 2015. pp. 51–8.
- Augustin A., Yi J., Clausen T., Townsley W., Augustin A., Yi J., et al. A Study of LoRa: Long Range & Low Power Networks for the Internet of Things. *Sensors.* 2016. **16**(9):1466.
- LoRa Alliance™* [Accessed: 5 April 2019]. Available from: <https://lora-alliance.org/>.
- Hadwen T., Smallbon V., Zhang Q., D'Souza M. Energy efficient LoRa GPS tracker for dementia patients. in: *2017 39th Annual International Conference of the IEEE Engineering in Medicine and Biology Society (EMBC).* 2017. pp. 771–4.
- Arduino* [Accessed: 5 April 2019]. Available from: <https://www.arduino.cc/>.
- Badamasi Y.A. The working principle of an Arduino. in: *2014 11th International Conference on Electronics, Computer and Computation (ICECCO).* 2014. pp. 1–4.
- OpenWRT* [Accessed: 5 April 2019]. Available from: <http://www.openwrt.org>.
- Benchmark of MQTT servers.* 2015.
- Farid M.M., Prawito, Susila I.P., Yuniarto A. Design of early warning system for nuclear preparedness case study at Serpong. in: *AIP Conference Proceedings.* 2017. p. 030067.
- Susila I.P., Yuniarto A., Cahyana C., Cahyana C. Monitoring and Analysis of Environmental Gamma Dose Rate around Serpong Nuclear Complex. *Atom Indones.* 2017. **43**(2):87.
- Susila I.P., Istofa, Kusuma G., Sukandar, Isnaini I. Development of IoT based meteorological and environmental gamma radiation monitoring system. in: *AIP Conference Proceedings.* 2018. p. 060004.
- Martinez B., Monton M., Vilajosana I., Prades J.D. The Power of Models: Modeling Power Consumption for IoT Devices. *IEEE Sens. J.* 2015. **15**(10):5777–89.
- Deepu C.J., Heng C.-H., Lian Y. A Hybrid Data Compression Scheme for Power Reduction in Wireless Sensors for IoT. *IEEE Trans. Biomed. Circuits Syst.* 2017. **11**(2):245–54.
- Seftelis I., Nicolaou G., Trassanidis S., Tsagas F.N. Diurnal variation of radon progeny. *J. Environ. Radioact.* 2007. **97**(2–3):116–23.
- Bencloski J.W. Air temperature and relative humidity: A simulation. *J. Geog.* 1982. **81**(2):64–5.

19. Lawrence M.G., Lawrence M.G. The Relationship between Relative Humidity and the Dewpoint Temperature in Moist Air: A Simple Conversion and Applications. *Bull. Am. Meteorol. Soc.* 2005. **86**(2):225–34.
20. Valsson S., Bharat A. Impact of Air Temperature on Relative Humidity - A study. *Archit. – Time Sp. People.* 2011.(February):38–41.